

## Three-dimensional optofluidic waveguides in hydrophobic silica aerogels via supercritical fluid processing

Gamze Eris<sup>a</sup>, Deniz Sanli<sup>a</sup>, Zeynep Ulker<sup>a</sup>, Selmi Erim Bozbag<sup>a</sup>, Alexandr Jonás<sup>b</sup>, Alper Kiraz<sup>b,c,\*\*</sup>, Can Erkey<sup>a,c,\*</sup>

<sup>a</sup> Department of Chemical and Biological Engineering, Koc University, 34450 Saryyer, Istanbul, Turkey

<sup>b</sup> Department of Physics, Koc University, 34450 Saryyer, Istanbul, Turkey

<sup>c</sup> Koç University TÜPRAŞ Energy Center (KÜTEM), Koç University, 34450 Saryyer, Istanbul, Turkey

### ARTICLE INFO

#### Article history:

Received 13 August 2012

Received in revised form 1 November 2012

Accepted 2 November 2012

#### Keywords:

Optofluidic waveguides

Trifluoropropyl POSS

Hydrophobic silica aerogel

Supercritical extraction

### ABSTRACT

Optofluidic components enable flexible routing and transformations of light beams in integrated lab-on-a-chip systems with the use of carefully shaped fluid parcels. For structural integrity reasons, the working fluid is typically contained within a solid-material chip. One of the outstanding challenges in optofluidics is the preparation and processing of optofluidic waveguides. These require solid cladding materials that are sufficiently strong to contain the fluid while possessing optical properties that allow efficient confinement of light within fluidic channels. Here, we report on a new technique to obtain liquid-core optofluidic waveguides based on total internal reflection of light in three-dimensional water-filled channels embedded in hydrophobic silica aerogel. To form the channels, we employ a fiber made of cage-like silicon-oxygen compound – trifluoropropyl polyhedral oligomeric silsesquioxane (trifluoropropyl POSS) – which has high solubility in supercritical CO<sub>2</sub> (scCO<sub>2</sub>). A U-shaped fiber made of trifluoropropyl POSS is obtained by melt/freeze processing of POSS powder and subsequently placed in a silicate sol. After gelation of the sol and aging of the gel, scCO<sub>2</sub> extraction is used to dry the wet gel and extract the POSS fiber, yielding a dry silica aerogel with a U-shaped empty channel inside it. Finally, the silanol groups at the surface of the aerogel are reacted with hexamethyldisilazane (HMDS) in the presence of scCO<sub>2</sub> to render the aerogel surface hydrophobic and the channel is filled with water. We demonstrate efficient waveguiding by coupling light into the water-filled channel and monitoring the channel output. The presented procedure opens up new possibilities for creating complex three-dimensional networks of liquid channels in aerogels for optofluidic applications.

© 2012 Elsevier B.V. All rights reserved.

### 1. Introduction

Optofluidics exploits unique properties of fluids for creating optical components and systems [1]. As fluids provide a great flexibility in shape and refractive index, and enable generation of optically smooth interfaces, they can be used for designing novel optical devices that cannot be realized with classical solid materials. In addition, optofluidic devices combined with microfluidic technologies pave the way for improved chemical and biological functionality in lab-on-a-chip analytical and preparative systems [2]. Examples of applications of integrated optofluidics include optical communication components, organic dye-based laser light sources, imaging systems, or biological sensors [3–5].

Optofluidic waveguides that serve for guiding and controlled routing of light beams are key components of lightwave circuits

with fluidic and optical elements integrated all on the same chip. Besides, they enable light-sample interactions over extended volumes that can be exploited in detection and sensing applications [2,4]. In order to confine and guide light, these waveguides exploit either interference or total internal reflection (TIR). In the former case, light undergoes multiple reflections from a periodic solid structure that confines the liquid and individual reflected waves subsequently interfere destructively or constructively. This principle is used in two-dimensional photonic crystal waveguides [6] and anti-resonant reflecting optical waveguides (ARROWS) [7]. In the latter case, waveguide core material with a high refractive index is surrounded by a waveguide cladding material with a low refractive index. This principle is used in solid core/liquid cladding waveguides, nanoporous-cladding waveguides and liquid core waveguides [8,9]. Since the waveguides based on TIR do not require fabrication of periodic reflective structures, they are generally easier to implement.

TIR-based liquid-core waveguides are composed of a liquid-filled channel in a solid material which acts as waveguide cladding. Cladding material should be non-absorbing and should have a

\* Corresponding author. Tel.: +90 212 3381866; fax: +90 212 3381548.

\*\* Corresponding author.

E-mail addresses: [akiraz@ku.edu.tr](mailto:akiraz@ku.edu.tr) (A. Kiraz), [cerkey@ku.edu.tr](mailto:cerkey@ku.edu.tr) (C. Erkey).

refractive index value  $n_{\text{cladding}}$  smaller than that of the core material ( $n_{\text{core}} > n_{\text{cladding}}$ ) in order to guide light with low attenuation. While  $n_{\text{core}} > n_{\text{cladding}}$  condition can be easily achieved for solid core waveguides, it becomes a challenge for liquid-core waveguides since refractive index of water and most aqueous solutions ( $n \sim 1.33$ ) is relatively low compared to solid materials used in microfluidic chip fabrication [5,9].

Hydrophobic silica aerogels are nanoporous materials which are prepared by supercritical drying of alcogels produced by the hydrolysis and condensation reactions of a silica precursor. Their physical properties can be tuned by changing the reactant concentrations and conditions used in the synthesis [10,11]. Silica aerogels with high porosity, high surface area and low density have been under investigation for use in a wide variety of applications such as thermal insulation, adsorption and drug delivery [12,13]. Silica aerogels also have the desired optical properties to be a good cladding material, in particular, high transparency and low refractive index around 1.05 at visible wavelengths [10]. This makes them attractive for optofluidic waveguiding applications.

Recently, optofluidic waveguides based on water-filled channels in silica aerogel blocks were demonstrated [14]. In that demonstration, a solid glass fiber was embedded into the silica sol and subsequently withdrawn after the aerogel synthesis, thus forming a channel. While this method is useful for fabricating straight channels, it is not suitable for the formation of curved channels or more complicated three-dimensional (3D) structures since the withdrawal of such structures from aerogel block would result in breakage of the aerogel. Furthermore, even withdrawal of straight fibers can cause aerogel damage due to the adhesion of the silica aerogel network to the fiber surface.

Hence, an alternative fabrication procedure needs to be developed for incorporation of complex 3D channel networks within the aerogel structure. One approach is to adopt a technique that is commonly used to induce pores in a wide variety of materials based on the leaching of solid particulates from a matrix [15]. If a silica aerogel can be prepared with a 3D object inside, which can then be extracted using a solvent, one would obtain a silica aerogel with a cavity inside having the shape of the 3D object. The success of such a strategy would depend on finding the appropriate cavity inducer-solvent combination. In the case of silica aerogels, conventional organic or aqueous solvents would not be suitable since the pores of the aerogels collapse when the aerogel is subjected to organic or aqueous solvents. However, supercritical extraction may be suitable for removal of solid objects from aerogels [16]. Recently,  $\text{scCO}_2$  extraction was used to make porous grinding wheels by the selective removal of  $\text{CO}_2$  soluble pore inducers from a matrix consisting of alumina, glass, binder and pore inducer. Moreover the pore size of the grinding wheels could be controlled by changing the size of the pore inducer particles [17]. Likewise,  $\text{scCO}_2$  soluble D-fructose particles were selectively removed using supercritical extraction to produce poly(L-lactic acid) (PLLA) scaffolds with macropores of 100–150  $\mu\text{m}$  which have good interconnectivity with each other and are thus suitable for tissue engineering applications [18]. Therefore, a suitable material needs to be found to make the 3D object which should be not only extractable using  $\text{scCO}_2$  but also be insoluble in the solvents used in the sol-gel process used to synthesize aerogels.

In this study, we present a new method to synthesize hydrophobic silica aerogels with an embedded U-shaped channel which serves as an optofluidic waveguide upon filling with water. In our method, we employed U-shaped fibers as a model for complex 3D networks since U-shaped fibers cannot be removed from the aerogel by pulling without breaking the aerogel and should be sufficient for demonstration of the developed technology. The fibers were prepared by melt/freeze processing of trifluoropropyl POSS powder. Millimeter-sized solid trifluoropropyl POSS fibers were

placed into the silica sol prior to gelation. Since trifluoropropyl POSS can be dissolved in  $\text{scCO}_2$ , the fibers were removed during the supercritical drying of silica alcogel with carbon dioxide, yielding a U-shaped hollow channel within the gel structure. Subsequently, the entire internal surface of the aerogel was made hydrophobic by reactive supercritical deposition involving reaction of hexamethyldisilazane (HMDS) with the surface silanol groups of silica aerogel. The channel was subsequently filled with water. We demonstrate efficient waveguiding by coupling light into the water-filled channel and monitoring the channel output.

## 2. Experimental

### 2.1. Chemicals

Trifluoropropyl POSS (Hybrid Plastics), TEOS (98% purity; Alfa Aesar), ethanol (99.9% purity; Merck), hydrochloric acid (HCl) (37% purity; Riedel-de Haen), ammonium hydroxide ( $\text{NH}_4\text{OH}$ ) (2.0 M in ethanol; Aldrich), and HMDS (Alfa Aesar 98%) were used as received.  $\text{CO}_2$  was obtained from Messer Aligaz and had a stated purity of 99.9%.

### 2.2. Trifluoropropyl POSS fiber preparation

Fibers used to obtain hollow channels in aerogels were prepared from trifluoropropyl POSS powder by melt/freeze processing. Initially, trifluoropropyl POSS powder was placed on a stainless steel plate which was selected due to its good heat conductivity and resistance to high temperatures. Subsequently, trifluoropropyl POSS powder was heated with a heat gun to a temperature above its melting point. The liquefied trifluoropropyl POSS was then accumulated uniformly around the back of a spoon forming a U-shaped fiber during solidification. Prior to final solidification at room temperature, the prepared fiber was removed from the spoon without damaging its structure.

### 2.3. Synthesis of silica aerogel with a U-shaped channel

Fig. 1 summarizes individual steps of synthesis of a silica aerogel containing a U-shaped channel. Silica aerogels were prepared using the conventional two step sol-gel procedure [13]. Tetraethylortho silicate (TEOS) was used as the silica precursor, HCl as the acid catalyst, and  $\text{NH}_4\text{OH}$  as the base catalyst. Initially, a solution was prepared by mixing TEOS, ethanol and water with the mass ratio 1:1:0.34 (Fig. 1a). Then, the acid catalyst was added (0.048 M in ethanol) in order to initiate the hydrolysis reaction and sol formation which was carried out for approximately 40 min (Fig. 1b). Subsequently, the base catalyst (0.1 M in ethanol) was added to the solution in order to increase the rate of condensation reactions. Before gelation, the solution was transferred into a plastic syringe-based mold with a diameter of 12.3 mm. U-shaped trifluoropropyl POSS fiber was placed in the solution in such a way that the curved part was inside the solution and the ends protruded from the upper surface (Fig. 1c). The fiber was held stationary until the solution in the mold transformed into a solid alcogel. This wet gel containing the trifluoropropyl POSS fiber was taken out from the mold after 20 min and displayed no cracks. The wet gel with the embedded fiber was then transferred into an aging solution consisting of equi-volume mixture of water and ethanol (Fig. 1d). The aging of the wet gel was performed at 323 K for 24 h. During this step, further condensation reactions occur that strengthen the wet gel. Subsequently, the ethanol-water solution was replaced with pure ethanol in which the alcogel was kept for 3 days to remove any impurities and water remaining in its pores (Fig. 1e).

Supercritical drying of the alcogel along with extraction of the embedded trifluoropropyl POSS fiber by  $\text{scCO}_2$  at 313.2 K and 9 MPa

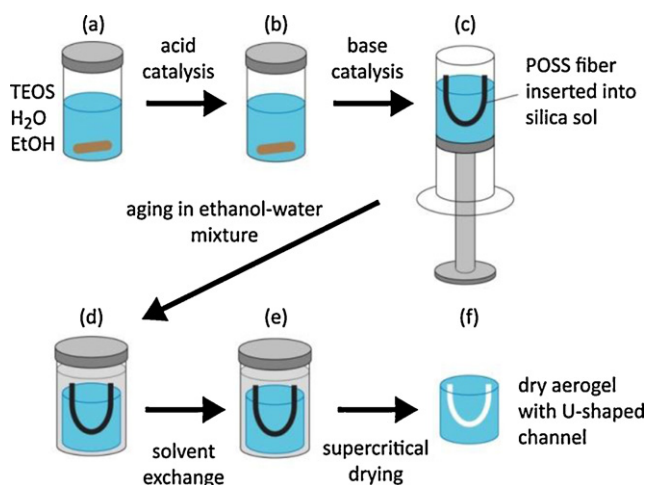


Fig. 1. Preparation of silica aerogel with an embedded U-shaped channel.

were performed using Applied Separations Speed SFE system. The condition was selected based on the protocols developed previously in our laboratory. In the first step, 26 mL extraction vessel was filled with ethanol to prevent contact of the sample with air and then alcogel was transferred into the vessel. Subsequently, ethanol from the gel pores and the embedded trifluoropropyl POSS fiber were extracted with  $\text{scCO}_2$ . Extraction was continued for a period of 8 h. Later, vessel was depressurized slowly (about 0.3 bar/min) to avoid formation of cracks. Extraction of the trifluoropropyl POSS fiber resulted in a U-shaped channel within the transparent silica aerogel (Fig. 1f). Even though the presence of ethanol is expected to decrease the solubility of trifluoropropyl POSS in  $\text{scCO}_2$ , the selected operating conditions and time were sufficient for complete removal of trifluoropropyl POSS from the gel [20].

#### 2.4. Surface modification with HMDS

Surface modification of silica aerogel containing an empty U-shaped channel with HMDS was performed in a high pressure vessel with an internal volume of 57 mL having two sapphire windows at each side (Fig. 2). A syringe pump (Teledyne ISCO Model: 260D) was used to transfer  $\text{CO}_2$  into the high pressure vessel. Pressure and temperature inside the vessel were measured using a pressure transducer and a thermocouple. The temperature of the vessel was controlled using a circulating heater (ColeParmer Polystat Circulating Bath). A magnetic stirrer was used to stir the contents of the vessel. Initially, a stainless steel screen was placed in the middle of the vessel in order to prevent the contact between

the aerogel and liquid HMDS. 1 mL of HMDS was placed at the bottom of the vessel while the aerogel was placed on top of the screen. The vessel was then sealed, filled with  $\text{CO}_2$  and brought to 333.2 K and 10.34 MPa. The operating temperature and pressure were selected on the basis of a previous study on the surface modification of silica aerogel by HMDS– $\text{CO}_2$  mixture [13]. All of the liquid HMDS dissolved in  $\text{CO}_2$  and the aerogel was left in contact with a solution of HMDS in  $\text{CO}_2$  for 2 h. After the treatment, supercritical extraction with pure  $\text{CO}_2$  was performed in order to remove the unreacted HMDS as well as the reaction products of HMDS with surface hydroxyl groups from the system. After the extraction, monolithic, crack-free and hydrophobic silica aerogel was obtained.

#### 2.5. Characterization of silica aerogels

The average pore size, the specific surface area as well as the micropore area were determined using nitrogen physisorption (Micromeritics ASAP 2020). First, samples were degassed at 353 K for 1 day to remove remaining impurities and solvent from the pores. Weight of the degassed samples was measured and then the pore analysis was performed using 60-point  $\text{N}_2$  adsorption/desorption isotherms with a relative pressure ( $P/P_0$ ) ranging from  $10^{-7}$  to 1 atm. The pore size distribution of the samples was determined using the Barret, Joyner and Halenda (BJH) method [19]. For the pore analysis, desorption branch of type II adsorption isotherm was used. Density of the samples was calculated by dividing the final mass of the silica aerogel by their final volume. Final volume was determined by measuring the physical dimensions of aerogel using a caliper. In order to characterize the changes in chemical composition of aerogels during their preparation Fourier transform infrared spectroscopy-attenuated total reflectance (FTIR-ATR) spectra of hydrophobic silica aerogel and trifluoropropyl POSS were acquired using an FTIR-ATR spectrometer (Thermo-Scientific Nicolet IS10). Water contact angle measurements based on direct imaging of surface-deposited water droplets were performed on HMDS-treated aerogels to quantify the hydrophobicity of the outer aerogel surface and the channel walls. Wetting properties of the channel walls were characterized by cutting the aerogel block along the channel and placing a water droplet directly on the channel surface.

#### 2.6. Characterization of optofluidic waveguides

U-shaped channels formed in hydrophobic silica aerogel blocks were filled with water by injection from a syringe. Because of the hydrophobicity of the aerogel surface, it was difficult to fill the channel with water. When a small pressure was applied to the syringe, some of the water was repelled and air bubbles were observed inside the channel. Applying a higher pressure to the syringe and a faster injection overcame water repellency and the channel could be filled with water. Excess water at the other end of the channel was wiped from the aerogel surface using a piece of paper towel.

Aerogel was placed on a two-dimensional translation stage for precise positioning and laser beam from a laser diode (wavelength 532 nm, maximal output power 35 mW) was focused at one end of the water-filled channel using a lens with a focal distance of 150 mm. The position of the beam focus in the channel cross-section could be adjusted using the translation stage. Subsequently, the intensity of light transmitted through the waveguide was visually monitored at the other end of the channel and the beam focus position was optimized for maximal transmission.

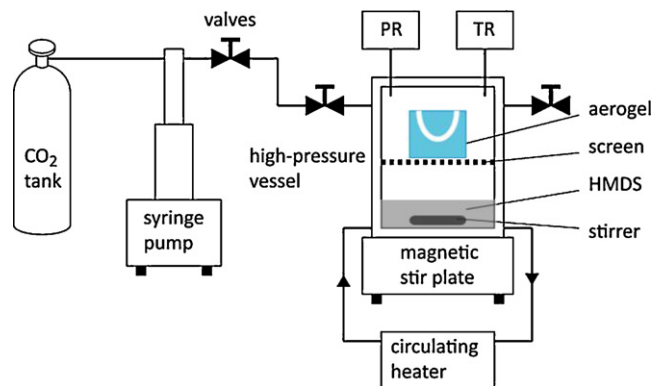


Fig. 2. Apparatus for silanization of the silica aerogel surface. PR, pressure readout; TR, temperature readout.

### 3. Results and discussion

A critical consideration in the development of our fabrication method was the selection of an appropriate material for producing the fiber that defines the shape of the channel in the aerogel. The fiber material should not be soluble in the aging solution (a mixture of water and ethanol) and in pure ethanol. On the other hand, it should be soluble in  $\text{scCO}_2$  since the fiber has to be removed during the supercritical drying process. First, a material satisfying the solubility criteria was searched. There are not many candidate compounds that are soluble in  $\text{scCO}_2$  but not soluble in solvents used in sol-gel processing to synthesize silica aerogels. A recent study indicated that trifluoropropyl POSS might be a good candidate since it was found to be quite soluble in  $\text{scCO}_2$  [20]. In this study, the cloud point pressure of trifluoropropyl POSS at 308 K and at a mole fraction of  $1.69 \times 10^{-3}$  was found to be 10.73 MPa. Subsequently, in order to find solubility of trifluoropropyl POSS in solvents used in the synthesis of silica aerogel, trifluoropropyl POSS powder was placed in pure water, pure ethanol and ethanol–water mixtures. It was found that trifluoropropyl POSS was insoluble in these solvents.

In addition to suitable solubility properties, one should be able to make a fiber out of the material by thermal processing. For that purpose, the material should melt at moderate temperatures which enable easy shaping into the fiber form and it should not turn into powder form upon cooling but should retain its shape. In the literature, we could find no reports on fibers made out of trifluoropropyl POSS. First, melting point of the trifluoropropyl POSS was measured with differential scanning calorimetry (DSC) as 460.2 K. Subsequent melting/cooling experiments showed that a uniform glassy structure could be obtained after heat treatment and subsequent cooling.

After the fiber was obtained successfully, an aerogel with the fiber inside was synthesized as described in the Section 2. The technique used to produce aerogel from alcogel was supercritical drying. In this technique, the high capillary pressures that act in conventional evaporation and lead to the collapse of gel pores are eliminated. Additionally, simultaneous drying of alcogel and removal of trifluoropropyl POSS fiber simplify the waveguide manufacturing procedure by reducing the number of necessary preparation steps. An important consideration in the process was extraction of the fiber from the aerogel without damaging the channel or the whole aerogel structure. During supercritical drying, shrinkage of the aerogel could potentially cause disruption of the channels due to additional generated stresses. Removal of fiber might also lead to the collapse of the channel. Nevertheless, very little shrinkage was observed during supercritical drying of the aerogels and uniform channels without any damage to the aerogel structure were consistently obtained. We believe that the weak interaction between trifluoropropyl POSS and silica surface was a crucial factor in obtaining crack-free aerogels. After performing silanization with HMDS, hydrophobicity of the aerogel was determined by measuring water contact angle on the silanized aerogel surface. Average contact angle determined from measurements at 8 different locations on the aerogel surface was  $140^\circ$  (see Fig. 3 for illustration). Measurements carried out on the channel walls provided similar values of the contact angle.

The typical properties of the aerogel pores were characterized using nitrogen physisorption. Average desorption pore radius was measured as 9.8 nm, surface area was measured as  $962 \text{ m}^2/\text{g}$  and pore volume was measured as  $4.3 \text{ cm}^3/\text{g}$ . These values are comparable to the previously published data [13].

FTIR-ATR spectroscopy was used to investigate the chemical composition of the HMDS-treated aerogel and determine if there was any trifluoropropyl POSS left at the surface of aerogel channels. To this end, FTIR-ATR spectra of powdered samples from hydrophilic silica aerogel and silanized surface of the aerogel

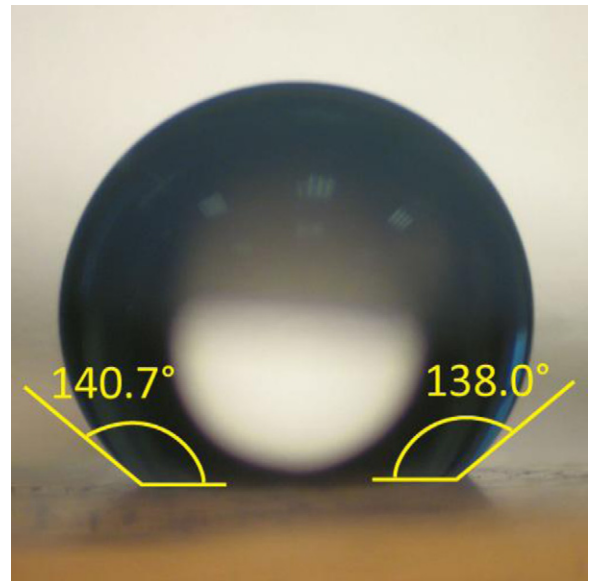


Fig. 3. Water droplet resting on the surface of hydrophobic silica aerogel.

channel along with the corresponding spectra of trifluoropropyl POSS powder were recorded. Fig. 4 presents the FTIR-ATR spectra of the aerogels and trifluoropropyl POSS. The peaks observed in the FTIR-ATR spectra of hydrophilic and hydrophobic silica aerogels were interpreted using the peak assignments for silica aerogel from a former study [21]. In the spectrum of hydrophilic silica aerogel (a), broad bands centered around  $960 \text{ cm}^{-1}$  and  $3400 \text{ cm}^{-1}$  represent stretching of surface silanol (Si–OH) groups. A strong and broad band at around  $1090 \text{ cm}^{-1}$  and a shoulder at around  $1200 \text{ cm}^{-1}$  correspond to Si–O–Si asymmetric stretching vibrations. Intense vibrations in that spectral region indicate the presence of a dense silica network. A peak at around  $800 \text{ cm}^{-1}$  is due to symmetric stretching vibrations of Si–O–Si. FTIR-ATR spectrum of hydrophilic aerogel (a) was compared with the FTIR-ATR spectrum of a sample obtained from the silanized surface of the channel inside the aerogel (b). The comparison indicates that the intensities of peaks at  $960 \text{ cm}^{-1}$  and  $3400 \text{ cm}^{-1}$  corresponding to Si–OH group were reduced and two new peaks emerged at

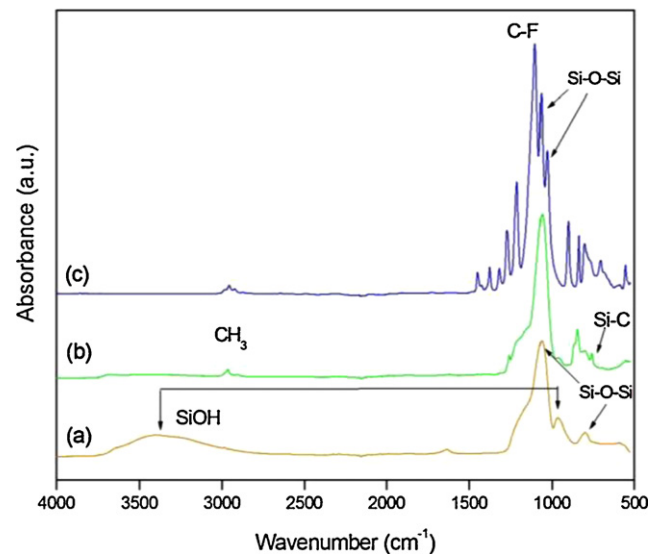
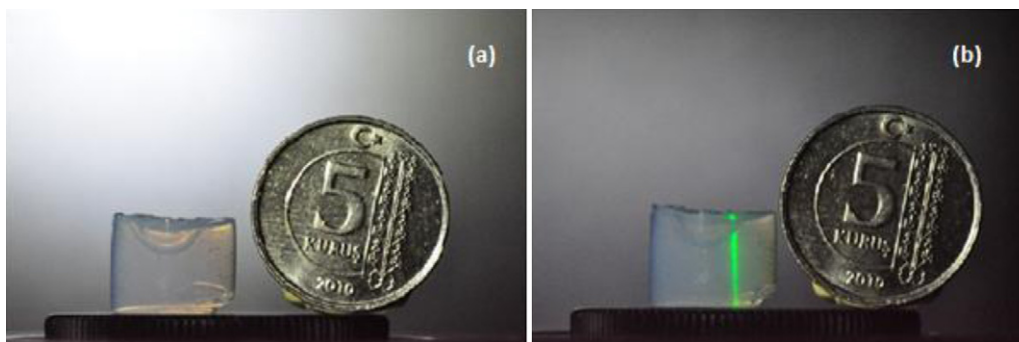


Fig. 4. FTIR-ATR spectra of (a) hydrophilic silica aerogel, (b) hydrophobic surface of the channel in silica aerogel, and (c) trifluoropropyl POSS.



**Fig. 5.** (a) Aerogel block with an empty U-shaped channel and (b) laser light focused from the top on one end of the channel before it was filled with water. Coin diameter is 17 mm.

837  $\text{cm}^{-1}$  and 2960–2975  $\text{cm}^{-1}$  corresponding to Si–C stretching vibrations and  $\text{CH}_3$  symmetric and asymmetric vibrations. These latter peaks reveal the products of reaction of HMDS with the silanol groups. A comparison was also done between the spectrum (b) and the spectrum of pure trifluoropropyl POSS (c). In the spectrum for trifluoropropyl POSS, the peak around 1100  $\text{cm}^{-1}$  is due to C–F stretching and the two peaks at 1060  $\text{cm}^{-1}$  and 1027  $\text{cm}^{-1}$  are due to Si–O–Si vibrations [22]. On the other hand, the peak corresponding to C–F vibrations, which is characteristic of trifluoropropyl POSS, is completely absent in the spectrum (b). Moreover, a number of sharp peaks between 1100  $\text{cm}^{-1}$  and 1470  $\text{cm}^{-1}$  present in the spectrum of trifluoropropyl POSS are not present in the spectrum of the sample from the aerogel channel surface. These results indicate that the concentration of trifluoropropyl POSS in the aerogel after supercritical extraction is below the detection limit of FTIR-ATR. In order to estimate the detection limit of the amount of trifluoropropyl POSS in the matrix, a 1 wt.% mixture of trifluoropropyl POSS with hydrophilic silica aerogel was prepared and its FTIR-ATR spectrum was acquired. The major peaks observed for pure trifluoropropyl POSS overlapped with the peaks of silica aerogel, however peaks of around 2900–3000  $\text{cm}^{-1}$  and 1500–1600  $\text{cm}^{-1}$  were observed in the mixture spectrum, thus showing that the detection limit for trifluoropropyl POSS is less than 1 wt.%. Hence, in combination with the analysis of the hydrophobic aerogel spectra of Fig. 4b, we can conclude that the residual concentration of trifluoropropyl POSS in the aerogel is well below 1%.

An image of aerogel synthesized by the above-described procedure is shown in Fig. 5a. A hollow U-shaped channel is clearly visible at the top part of the aerogel block. Due to the absence of water in the channel, green laser beam that was coupled into the right channel opening from the top was transmitted through the aerogel without any light guiding (see Fig. 5b). The path of the laser beam through the aerogel was visible due to the scattering of light from the aerogel network. Subsequently, the channel was filled with water and the light coupling experiment was repeated. In this case, laser light coupled into the right end of the channel was observed to be guided along the channel before exiting from the left end (see Fig. 6b). When the beam focus was moved outside of the channel cross-section, the laser beam was again transmitted straight through the aerogel without any light guiding, similarly to the case of an empty channel (compare Fig. 6a and Fig. 5b).

A side-top view of a water filled channel with laser light coupled into the left end of the channel is presented in Fig. 7. A bright green spot at the right end of the channel indicates light transmitted through the liquid-core optofluidic waveguide; this light propagates along a curved path with the radius of curvature of approximately 3 mm. Images of aerogel with water-filled channel and laser beam coupled into the channel show no substantial waveguide loss due to the light scattering from the channel walls (compare Fig. 6a and b for the intensity of non-guided light

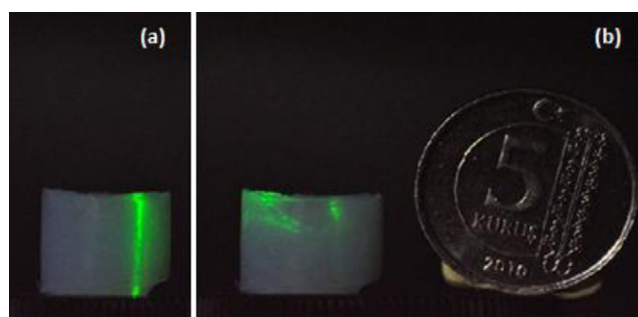


**Fig. 6.** (a) Laser light focused from the top on the aerogel block outside of a water-filled channel and (b) laser light focused from the top on the right end of the water-filled channel. Coin diameter is 17 mm.

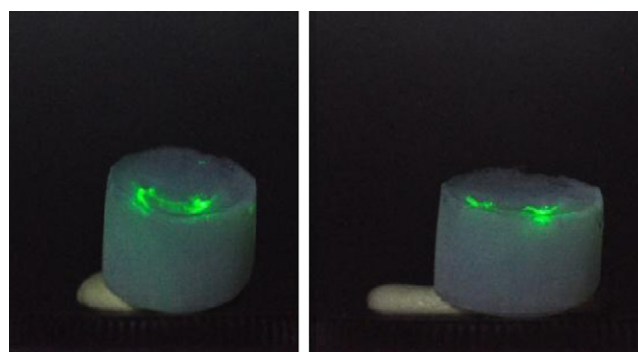


**Fig. 7.** Light guiding in a water-filled channel inside aerogel. The light was focused on the left end of the channel and exited from the right end of the channel.

scattered from the aerogel). Due to the U-shaped geometry of the liquid channel and high divergence angle of the light transmitted through the channel, it was not possible to measure directly the fraction of transmitted power. Currently, we are working on the preparation of L-shaped channels that would allow collecting the transmitted light with an integrating sphere and, thus, characterizing quantitatively the performance of the optofluidic waveguide.

In our experiments, we did not observe water penetration into the aerogel pores; we attribute this to the hydrophobic nature of the HMDS-treated aerogel surface (measured water contact angle  $> 140^\circ$ ). Repeated measurements performed over several weeks revealed no significant aging in the produced structures when water was dried following each measurement. Aging is, however, expected when water is kept in the channel for prolonged times.

#### 4. Conclusion

We obtained curved optofluidic waveguides by forming water-filled channels within hydrophobic silica aerogels. The channels were produced by the removal of a fiber made out of trifluoropropyl POSS during the  $\text{scCO}_2$  drying step of aerogel preparation. We observed light guiding in the channels upon laser light coupling. Our process is capable of producing optofluidic networks of any three-dimensional geometry prepared from trifluoropropyl POSS, including more complicated structures such as spherical water-filled optical resonators. Minimum size of the produced optofluidic networks can be further reduced by decreasing the dimensions of the objects made out of trifluoropropyl POSS. Thus, the presented procedure opens up new possibilities for creating complex three-dimensional networks of liquid channels in aerogels for optofluidic applications. Furthermore, the demonstrated use of trifluoropropyl POSS in conjunction with  $\text{scCO}_2$  processing may pave the way for development of other interesting applications in materials science.

#### Acknowledgement

We are grateful for the support of Koç University TÜPRAŞ Energy Center (KÜTEM).

#### References

- [1] D. Psaltis, S.R. Quake, C.H. Yang, Developing optofluidic technology through the fusion of microfluidics and optics, *Nature* 442 (2006) 381–386.
- [2] D. Brennan, J. Justice, B. Corbett, T. McCarthy, P. Galvin, Emerging optofluidic technologies for point-of-care genetic analysis systems: a review, *Analytical and Bioanalytical Chemistry* 395 (2009) 621–636.
- [3] Y. Fainman, L. Lee, D. Psaltis, C. Yang, *Optofluidics: Fundamentals, Devices, and Applications*, McGraw-Hill, New York, 2010, pp. 59–74.
- [4] C. Monat, P. Domachuk, B.J. Eggleton, Integrated optofluidics: a new river of light, *Nature Photonics* 1 (2007) 106–114.
- [5] D. Li, *Encyclopedia of Microfluidics and Nanofluidics*, Springer, New York, 2008, pp. 1573–1572.
- [6] M. Loncar, D. Nedeljkovic, T. Doll, J. Vuckovic, A. Scherer, T.P. Pearsall, Waveguiding in planar photonic crystals, *Applied Physics Letters* 77 (2000) 1937–1939.
- [7] R. Bernini, S. Campopiano, L. Zeni, P.M. Sarro, ARROW optical waveguides based sensors, *Sensors and Actuators B: Chemical* 100 (2004) 143–146.
- [8] H. Schmidt, A.R. Hawkins, Optofluidic waveguides: I. Concepts and implementations, *Microfluidics and Nanofluidics* 4 (2008) 3–16.
- [9] A.R. Hawkins, H. Schmidt, Optofluidic waveguides: II. Fabrication and structures, *Microfluidics and Nanofluidics* 4 (2008) 17–32.
- [10] A.S. Dorcheh, M.H. Abbasi, Silica aerogel; synthesis, properties and characterization, *Journal of Materials Processing Technology* 199 (2008) 10–26.
- [11] M.A. Aegerter, N. Leventis, M.M. Koebel, *Aerogels Handbook*, Springer, New York, 2011, pp. 21–74.
- [12] L.W. Hrubesh, Aerogel applications, *Journal of Non-Crystalline Solids* 225 (1998) 335–342.
- [13] S. Giray, T. Bal, A.M. Kartal, S. Kizilek, C. Erkey, Controlled drug delivery through a novel PEG hydrogel encapsulated silica aerogel system, *Journal of Biomedical Materials Research Part A* 100A (2012) 1307–1315.
- [14] L.M. Xiao, T.A. Birks, Optofluidic microchannels in aerogel, *Optics Letters* 36 (2011) 3275–3277.
- [15] C.J. Liao, C.F. Chen, J.H. Chen, S.F. Chiang, Y.J. Lin, K.Y. Chang, Fabrication of porous biodegradable polymer scaffolds using a solvent merging/particulate leaching method, *Journal of Biomedical Materials Research* 59 (2002) 676–681.
- [16] J.L. Gurav, I.K. Jung, H.H. Park, E.S. Kang, D.Y. Nadargi, Silica aerogel: synthesis and applications, *Journal of Nanomaterials* 2010 (2010).
- [17] T.D. Davis, J. Di Corleto, D. Sheldon, J. Vecchiarelli, C. Erkey, A route to highly porous grinding wheels by selective extraction of pore inducers with dense carbon dioxide, *Journal of Supercritical Fluids* 30 (2004) 349–358.
- [18] E. Reverchon, S. Cardea, C. Rapuano, A new supercritical fluid-based process to produce scaffolds for tissue replacement, *Journal of Supercritical Fluids* 45 (2008) 365–373.
- [19] E.P. Barrett, L.G. Joyner, P.P. Halenda, The determination of pore volume and area distributions in porous substances: computations from nitrogen isotherms, *Journal of American Chemical Society* 73 (1951) 373–380.
- [20] C. Dilek, Supercritical carbon dioxide-soluble polyhedral oligomeric silsesquioxane (POSS) nanocages and polymer surface modification, *The Journal of Supercritical Fluids* (2012), <http://dx.doi.org/10.1016/j.supflu.2012.10.012>.
- [21] R. Al-Oweini, H. Ei-Rassy, Synthesis and characterization by FTIR spectroscopy of silica aerogels prepared using several  $\text{Si}(\text{OR})_4$  and  $\text{R}'\text{Si}(\text{OR})_3$  precursors, *Journal of Molecular Structure* 919 (2009) 140–145.
- [22] J. Coates, Interpretation of infrared spectra, a practical approach, in: R.A. Meyers (Ed.), *Encyclopedia of Analytical Chemistry*, John Wiley & Sons Ltd., Chichester, UK, 2000, pp. 10815–10837.